Wind-solar complementarity and effective use of distribution network capacity

Wei Sun*, Gareth P. Harrison*

School of Engineering, University of Edinburgh, Mayfield Road, Edinburgh EH9 3DW, UK

HIGHLIGHTS

- Network wide impact of deploying hybrid combinations of renewables studied.
- Multi-period optimisation configures renewable capacity to maximise energy export.
- Combination of resources leads to more effective use of network capacity.
- Value of complementarity compounded by network topology, control and demand.
- Combined benefit of hybrid generation with active network management is identified.

ARTICLE INFO

ABSTRACT

Exploiting the diversity between different renewable resources is regarded as a significant tool to managing their grid integration. Hybrid combinations of resources provide the potential to smooth output and so overcome limits on the export of power, but their network wide impact is not well understood. This paper examines whether combinations of renewable distributed generation can make more effective use of distribution network capacity. A multi-period, multi-resource optimal power flow approach is used to optimally configure wind and solar photovoltaic capacity to maximise energy production whilst complying with network physical limits. The effectiveness of hybrid distributed generation and the optimization method was examined through comparison with cases using single types of renewable distributed generation. This study demonstrates that by capturing the complementarity between renewables through hybrid design, the network can host more renewable generation capacity and increase total energy export. In addition, smart grid techniques, such as active network management, further boosts the value of resource diversity by allowing connection of more generation capacity of all considered renewables through isolating the infrequent co-occurrence of high outputs during periods of low electricity demand.

1. Introduction

Renewable generation from wind, solar photovoltaics (PV) and hydro is growing rapidly to meet ambitious targets for carbon emissions reduction [1]. Connecting renewable generators into power grids typically occurs in the distribution network, as distributed generation (DG). This can be a challenging exercise as these grids were generally designed to supply power from the transmission network via a grid supply point (GSP) to customers at medium and low voltages. Distribution network operators are concerned with a range of technical criteria that can be affected by the connection of DG: voltage rise, reverse power flows, increased fault levels, power quality and system stability [2]. The strict technical limits on these factors serve to limit

the capacity of DG that may be connected to the network or necessitates expensive network reinforcement in order to raise capacity.

Reverse power flows and voltage rise are generally the major issue [3]. These arise due to the changes in power flows following DG connection. Without DG, power flows through lines and transformers towards the load with flows following the pattern of demand. Voltage reduces in the direction of power flows through the network and more significant voltage drops are seen under high demand conditions. Once DG is connected, lower levels of DG output may be sufficient to supply local loads, reducing the power flows through the network. However, larger output will exceed the local load and power is exported back towards the transmission network; if these reverse flows are sufficiently large they can exceed the power flow capability of lines and

* Corresponding authors.
E-mail addresses: W.Sun@ed.ac.uk (W. Sun), Gareth.Harrison@ed.ac.uk (G.P. Harrison).

Nomenclature

Acronyms

ACOPF	Alternating current optimal power flow
ANM	Active network management
DG	Distributed generation
HRES	Hybrid renewable energy systems
GSP	Grid supply point
OLTC	On-load tap changers
PV	Photovoltaic
NLP	Nonlinear program

Sets and indices

B, b	Set/index of electrical buses
G, g	Set/index of all DG
G_b	Set of generators connected to bus b
L, l	Set/index of power lines (and transformers)
M, m	Set/index of time periods
R, r	Set/index of renewable types
X, x	Set/index of external connections
X_b	Set of external supplies connected to bus b
β_l^1, β_l^2	Bus at each end of line ($\beta_l^{1,2} \in B$)

Variables

$f_{l,m}^{1,P}, f_{l,m}^{2,P}$	Active power injections at each end of line (MW)
$f_{l,m}^{1,Q}, f_{l,m}^{2,Q}$	Reactive power injections at each end of line (Mvar)
$p_{b,m}^l, q_{b,m}^l$	Active/reactive power injections into line l at b (MW, Mvar)
$p_{r,g}$	Installed capacity of DG for renewable type r (MW)
$p_{r,g,m}^{curt}$	Curtailment of power output for renewable type r (MW)
$p_{x,m}, q_{x,m}$	Active/reactive power flow through external supply source (MW, Mvar)
$V_{b,m}$	Bus voltage magnitude (p.u.)
$V_{OLTC,m}$	Voltage at transformer secondary bus (p.u.)
$\delta_{b,m}$	Bus voltage angle (°)

Parameters

b_0	Reference (slack) bus
d_b^P, d_b^Q	Peak active/reactive bus demand (MW, Mvar)
f_l^+	Apparent power flow limit of line (MVA)
P_x^+, P_x^-	Active power flow limit at GSP (MW)
Q_x^+, Q_x^-	Active power flow limit at GSP (Mvar)
V_b^+, V_b^-	Max/min voltage limit of bus (p.u.)
V_{OLTC}^+, V_{OLTC}^-	Max/min voltage limit of transformer secondary bus (p.u.)
τ_m	Duration of time period (h)
ω_m	Potential generation level at time period m for renewable type r
λ_r^{curt}	Maximum curtailment level
η_m	Demand level relative to its peak value in period m
$\phi_{g,m}$	Power factor angle of generator (°)

transformers [4]. By reducing flows, smaller DG output tends to reduce the extent of voltage drop but the reversal in flow at high output means voltage can be higher at the DG than the GSP. Should DG become too large then voltage may rise above the allowed limits. The output of renewable DG also varies and this sets an upper limit to the capacity of DG that can be connected. This is normally the 'firm' capacity at which maximum DG output can be exported at any time. This tends to occur during maximum generation output and minimum demand levels as this sees the highest reverse power flow and voltage rise. With renewable generation, these conditions tend to occur relatively infrequently, meaning that firm capacity could limit the ability of a network for connecting renewable generation based on conditions in a few hours a year [5]. As such it is the combined *variability* of demand and renewable generation that is important in defining capacity and ultimately the energy produced.

One way to ease the shortcomings of variability is to exploit the complementarity among different renewable sources through portfolio effects. Many studies report mutual complementarity of multiple renewable resources across large geographic areas including Italy [6], Britain [7], Canada [8] and China [9]. This can be captured by 'hybrid' renewable energy systems (HRES) which can be any combination of generation from two or more renewable and/or conventional resources [10], that work standalone or grid-connected. A considerable amount of work has been carried out on HRES, demonstrating that they can improve efficiency, reliability and facilitate greater energy production.

The design of HRES focusses on the optimization of the capacities of different renewables along with storage and/or conventional generation as support. Studies have mainly focused on off-grid applications employing different optimisation techniques including probabilistic [11], iterative [12,13] and artificial intelligence approaches [14]; all report reduced system costs and reliable supply. Recent studies include improved particle swarm optimisation with strong computational performance [15] and robust multi-objective optimization to handle renewable uncertainty [16]. With the development of smart grids, increasing attention has been paid to grid-connected hybrid systems, using grid supply as backup in case of deficiency while selling surpluses

to improve system economics. Grid-connected HRES is optimally sized in [17] using a genetic algorithm coupled with sensitivity analysis. Constraint-based iterative search algorithms are used in [18] to obtain optimal sizes with both maximum reliability and minimum cost. The effect on reducing carbon emissions from grid-connected hybrid systems is studied in [19] while the uncertainty of power exchanges between grid and HRES in optimal scheduling is tackled with stochastic multi-objective programming in [20]. All of the studies above are either off-grid or grid-connected at a single location. There is little work explicitly looking at the *network-wide* impact of deploying co-located hybrid combinations of resources to multiple locations at distribution level, and, more specifically, the value of integrating these from the point of view of efficient use of network capacity. With DG a common term in distribution network studies, grid-connected HRES will be generally referred to in this paper as 'hybrid DG'.

A second approach to handling variability is exploiting the potential for smart grids with active Network Management (ANM) a particular focus at distribution level [21]. The scope for ANM to make the best use of existing network capacity for accommodating (or 'hosting') renewable generation and avoiding costly reinforcement is widely recognised [22]. It does this by coordinating controls between network equipment and DGs to enable greater overall output within the network operational limits. In doing so, it facilitates larger generators to be connected than would otherwise be possible with traditional network practice. ANM includes voltage control using transformer on-load tap changers (OLTC) [23], active output control (i.e. power curtailment) [24], network reconfiguration [25], and may involve energy storage [26] and demand side management [27]. However, much of the ANM work has been envisaged in networks with single, non-hybrid renewable types. With ANM enhancing the network-side control while hybrid systems smooth out variable production on the generation side, they appear to be a good match for increasing renewable energy deployment. Nevertheless, the value of ANM and hybrid DG has not been explicitly examined in terms of the effective use of network capacity.

Examining how prospective connections of DGs with multiple resource types may influence effective use of network capacity is

complex. Identifying where opportunities exist within the distribution network to connect hybrid DG is a nonlinear optimisation exercise that requires detailed assessments of power flows to capture the key network operational constraints such as bus voltages and the thermal loading of feeders. These values depend on renewable availability at each location, typically requiring a long study horizon to capture a wide range of potential meteorological conditions that might occur, yet employing relatively short time steps (e.g. hourly) to accurately capture the renewable variability. The need to model the complementarity between multiple renewables in detail, as well as, account for critical nonlinear features such as network voltage profiles, makes such analysis challenging.

Given the research gap and challenges, this paper employs a multi-period, multi-resource optimal power flow-based assessment methodology to evaluate how hybrid DG with combinations of renewables influence the effective use of the network: the 'hosting capacity'. To our knowledge, this is the first paper that quantifies the network-wide benefit of hybrid DGs and the joint value with smart grid approaches. Its primary contribution lies in highlighting that diversity between renewables has 'value' in terms of being able to better exploit network capacity (i.e. 'fill' the network) and that this effect becomes more pronounced when active network management is employed. A secondary aspect of the novelty lies in the technique for combining multiple renewable resource time series in order to make computation more accessible.

The paper is organised as follows: Section 2 describes the methodology for evaluating the value of hybrid distributed generation in terms of maximizing energy production and effective use of network capacity. In Section 3 results for planning hybrid wind and PV DGs in a typical UK distribution network are presented and discussed. The remainder of the paper discusses and concludes the work.

2. Modelling methodology

2.1. Assessing hybrid renewable DG for effective use of network capacity

The connection of renewable DG in electricity networks needs to ensure that the network can physically handle power flows within defined technical and equipment limits. Optimal power flow (OPF) is a standard tool in electrical power systems and has traditionally been used for economic dispatch and operational planning. OPF is an optimisation problem formulated and solved to obtain optimal control settings such as the required power output of a given generator whilst respecting important system limits such as power line ratings. The most accurate OPF uses the full alternating current 'AC' formulation ('ACOPF') which, by considering both active and reactive power flows, accurately models the voltage profile throughout the network. This is critical in distribution networks as voltage levels are driven by both active (MW) and reactive (Mvar) power flows and voltage limits are normally the most significant constraint on capacity. ACOPF is a complex non-linear problem (NLP) with non-linear constraints.

ACOPF has also found application in a 'planning' setting including in identifying where generation capacity may be located without the need to reinforce the network (hosting capacity) [4,28]. Specifically, this means identifying the capacities that are feasible at one or more network buses (nodes). The time variability of renewable generation makes identification of capacity more challenging, particularly with multiple resources with different operational patterns. To handle this, the standard ACOPF is extended to a multi-period multi-resource approach to optimise the configuration of generation capacities over multiple renewable resources.

Mathematically, the objective of the optimisation is to maximise overall energy production from hybrid renewable DG within the constraints imposed by the existing network. This objective is chosen as it provides a measure of efficient use of overall network capacity but with the view that the energy generation is the valuable product not capacity

per se. The maximum production is obtained by optimally siting and sizing capacities for each resource r (R, set of renewable types), whilst accounting for the time variability and coincidence of demand and generation levels. The objective is given as:

$$\max \sum_{m \in M} \sum_{r \in R} \sum_{g \in G_b} p_{r,g} \omega_{r,m} \tag{1}$$

where $p_{r,g}$ is the (active) power capacity of generator g for renewable type r; G_b is the set of generators connected to bus b (B, set of buses); $\omega_{r,m}$ is the generator output level relative to its peak value as dictated by the renewable resource r in period m (M, the set of time periods). At each location a generator can be made up from one or more renewable resource types. The problem then seeks to find a unique and optimal set of capacities $p_{r,g}$ of hybrid DGs at all prospective connection buses, which deliver the maximum energy over all periods in the study period M. While based on the same broad framework as [24], the objective function, application, use of multiple renewable resources and specific details of the formulation are quite distinct. The specific technique used to combine multiple renewable resource time series in order to make computation more accessible is detailed in Section 2.4.

2.2. Network constraints

The objective of maximising energy production from multiple DGs is subject to a set of constraints representing those that govern the physical operation of the networks (e.g. nodal power balance) and limits imposed by statute and standards (e.g. voltage limits) as well as equipment ratings (e.g. power flow limits).

(1) Active and reactive nodal power balance:

The physical nodal balance of electricity power flow is enforced by Kirchhoff's current law for each bus in the network, which states that current flowing into a node must match that flowing out. The nodal power balance for active power is given by:

$$\sum_{l \in L \mid \beta_l^{1,2} = b} p_{b,m}^L + d_b^P \eta_m = \sum_{g \in G_b} \sum_{r \in R} p_{r,g} \omega_{r,m} + \sum_{x \in X_b} p_{x,m} \quad \forall\, b$$
$$\in B, \forall\, m \in M \tag{2}$$

where $p_{b,m}^L$ is the total active power injection into lines (and transformers) at bus b, and η_m is the demand level in time period m relative to bus peak active power demand d_b^P. The distribution network is ultimately connected to external networks such as the transmission network through a grid supply point substation. This acts to balance the distribution network by allowing imports or exports of excess generation; $p_{x,m}$ is the active power imported/exported from external connections x (X_b, set of external supplies).

A similar relationship governs the reactive power nodal balance:

$$\sum_{l \in L \mid \beta_l^{1,2} = b} q_{b,m}^L + d_b^Q \eta_m = \sum_{g \in G_b} \sum_{r \in R} p_{r,g} \omega_{r,m} \tan(\phi_{r,g,m}) + \sum_{x \in X_b} q_{x,m} \quad \forall\, b$$
$$\in B, \quad \forall\, m \in M \tag{3}$$

where $q_{b,m}^L$ are the total power reactive power injections into lines; d_b^Q are the bus peak reactive demands; $q_{x,m}$ is the reactive power supplied to/from external connections; and $\phi_{g,m}$ are the generator power factor angles.

The power flow requires one bus to act as the reference in order to ensure overall balance. The higher voltage side of the GSP substation is taken as the reference bus b_0 with the voltage angle set at zero, $\delta_{b_0,m} = 0$. The constraints on import and export of active and reactive power flow through the GSP are given by:

$$P_x^- \leqslant p_{x,m} \leqslant P_x^+$$
$$Q_x^- \leqslant q_{x,m} \leqslant Q_x^+ \quad \forall\, x \in X, \ \forall\, m \in M \tag{4}$$

where $P_x^{(+,-)}$ and $Q_x^{(+,-)}$ are the active and reactive flow limits.

(2) Voltage level limits:

Voltage rise at or near renewable DG connection points is one of the

major issues for network operators. Voltages at network bus b are constrained by the maximum and minimum allowed levels $V_b^{(+,-)}$:

$$V_b^- \leqslant V_{b,m} \leqslant V_b^+, \quad \forall b \in B, \quad \forall m \in M \tag{5}$$

Voltages are typically described relative to their nominal voltage level using the per unit scale (p.u.). For example, a voltage of 11,550 V on an 11 kV line would be recorded as 1.05p.u. or $+5\%$ of nominal. Voltage limits are defined on a percentage of nominal basis, e.g. $\pm 6\%$.

(3) Power flow limits:

Equipment ratings constrain overall power flow through lines and transformers, l (L, set of lines):

$$(f_{l,m}^{(1,2),P})^2 + (f_{l,m}^{(1,2),Q})^2 \leqslant (f_l^+)^2, \quad \forall l \in L, \forall m \in M \tag{6}$$

where f_l^+ is the apparent (i.e. total active and reactive) power flow limit of the lines. $f_{l,m}^{(1,2),P}$ and $f_{l,m}^{(1,2),Q}$ are the active and reactive power injections at each end of the line (denoted 1 and 2) as standard Kirchhoff voltage law expressions. These provide the fundamental link between power flows within lines and voltages at buses; further details can be found in any good power systems textbook.

2.3. Boosting hybrid systems using active network management

The integration of hybrid combinations of resources may be able to exploit the capability of ANM alongside potential advantages of production diversity. A wide range of relevant ANM techniques are available and can be readily incorporated, but to illustrate this two ANM schemes are modelled within the optimisation: adaptive voltage control and active output control (i.e. production curtailment).

2.3.1. Adaptive voltage control

Active exploitation of the voltage regulation function provided by the on-load tap changers on transformers is often proposed to mitigate voltage rise. Traditional use of OLTC requires a defined setpoint voltage to be specified for the secondary (low voltage) bus that the OLTC aims to meet by adjusting the winding ratio on the transformer. The setpoint value is normally specified for entire seasons or years. Adaptive voltage control involves actively modifying the target voltage of the OLTC according to the conditions at a particular point in time instead of using a single predefined target voltage across all time periods.

In the modelling framework here, the secondary (low) voltage bus at the substation transformer is dynamically controlled by the OLTC in each period so as to ensure all the voltages along the feeders are within allowable limits. It is treated as a variable, $V_{OLTC,m}$ maintained within a range V_{OLTC}^- to V_{OLTC}^+, rather than as a fixed parameter. This is handled as a constraint within the multi-period OPF formulation:

$$V_{OLTC}^- \leqslant V_{OLTC,m} \leqslant V_{OLTC}^+ \tag{7}$$

In general, the optimisation will raise voltage $V_{OLTC,m}$ at the transformer when demand is high and DG production low to avoid under voltages at the edges of the network, while lowering it when DG production is high and demand low to avoid over voltages.

2.3.2. Active output control

Without ANM, most renewable generators are provided with a 'firm' connection at present, where DG can freely operate up to its rated output albeit limited by the weather conditions. The limiting factor is generally the worst-case scenario of low demand and high renewable output. Due to the infrequent occurrence of these, firm connection arrangements could unnecessarily limit the hosting capacity of a network for connecting renewable generation. Active control of DG production provides a general solution for connecting capacity above the firm capacity level by reducing (i.e. curtailing) generation output during low demand periods ensuring that network parameters remain within limits. While this may involve lost revenue for the DG, this may be acceptable to the developer as it enables larger generators to be

connected, increasing the overall energy production and total revenue.

The curtailment scheme is formulated as a time-dependent variable $p_{r,g,m}^{curt}$ which defines the necessary curtailed generation for each renewable component r of generator g in period m. In the original power balance Eqs. (2) and (3), delivered power generation matches the potential generation $\sum_{r \in R} p_{r,g} \omega_{r,m}$. Here, actual delivered energy is reduced by the amount curtailed, $\sum_{r \in R} (p_{r,g} - p_{r,g,m}^{curt}) \omega_{r,m}$ and the balance equations are changed to:

$$\sum_{l \in L | \beta_l^{1,2} = b|} p_{b,m}^L + d_b^P \eta_m = \sum_{g \in G_b} \sum_{r \in R} (p_{r,g} - p_{r,g,m}^{curt}) \omega_{r,m} + \sum_{x \in X_b} p_{x,m} \quad \forall b$$
$$\in B, \ \forall m \in M \tag{8}$$

$$\sum_{l \in L | \beta_l^{1,2} = b} q_{b,m}^L + d_b^Q \eta_m = \sum_{g \in G_b} \sum_{r \in R} (p_{r,g} - p_{r,g,m}^{curt}) \omega_{r,m} \tan(\phi_{g,m})$$
$$+ \sum_{x \in X_b} q_{x,m} \quad \forall b \in B, \ \forall m \in M \tag{9}$$

By its physical meaning, the curtailment $p_{r,g,m}^{curt}$ for each renewable DG should not exceed the full potential output in the corresponding period:

$$p_{r,g,m}^{curt} \leqslant p_{r,g} \omega_{r,m}, \quad \forall r \in R, \forall g \in G, \forall m \in M \tag{10}$$

Economic considerations will ultimately limit the total amount of curtailed energy that will be acceptable to the owner of renewable generators. These are strongly dependent on the network connection arrangements where different 'principles of access' govern the order and extent of curtailment between DGs [29]. This is an evolving area and complex in its own right so here a simplified approach is taken which places an upper limit on the amount of curtailment that is allowed. A curtailment factor λ_g^{curt} is applied as a constraint restricting the proportion of the total potential energy at each location that could have otherwise been delivered over the whole period:

$$\sum_{m \in M} \sum_{r \in R} p_{r,g,m}^{curt} \tau_m \leqslant \lambda_g^{curt} \left[\sum_{m \in M} \sum_{r \in R} p_{r,g} \omega_{r,m} \tau_m \right], \quad \forall g \in G \tag{11}$$

The optimisation chooses the precise split in curtailment between different resources at each location in relevant periods. There are alternative ways of applying a constraint on curtailment and the effect of these are considered in the Section 3.7.

2.4. Framework for handling variable renewables

Ideally, the nonlinear ACOPF formulation of (1)-(6) would directly use a long time-series of renewable and demand data, so that the analysis captures the full range of varying operational conditions. This study period M should be a year (and preferably much longer), however, this introduces a significant number of time-varying variables and correspondingly additional constraints into the nonlinear program. For example, a set of half-hourly data for 1 year will generate 17,520 periods of network operation to be considered simultaneously so as to find a unique inter-temporal solution in the nonlinear optimization. Therefore, an explicit long-term time-series study on even a relatively small section of the distribution network results in a large computational burden which tends to be laborious or intractable. As such, evaluating distribution network capacity requires a means of effectively dealing with the problems of multi-dimensionality introduced by renewable variability, without unduly increasing the associated computational burden.

To mitigate the computational burden, a process is used to discretise and then aggregate according to the characteristics of 'similar' periods. In essence this reduces the number of discrete periods to be evaluated whilst preserving the behaviour and inter-relationships between multiple resources and demand. Such treatment of long-term time-series data is first proposed by Ochoa et al. [24] although only wind was

considered. The further development of the multi-period approach in this paper addresses the 'coincidence' of *multiple* renewable resources with electrical demand.

The discretisation process allocates original data values for resources and demand into a series of bins covering the range between zero and overall peak value. To illustrate this, Fig. 1(a) presents a two day-long snapshot of hourly demand and wind power data [30] with values expressed as percentage of respective peak values. For each set of data, the hourly values are compared with and assigned to one of 7 bin ranges – {0}, (0,20%], (20%,40%],…, (80%,100%), {100%} – with the mean value of the range characterising each hour (e.g., 30% for the (20%,40%] range). Fig. 1(b) shows the resulting time series. The choice of bin is flexible but the ranges shown here are deliberately wide and much narrower ranges will allow values to be closer to original values. The discretisation process can be carried out for any number of resource and demand time series.

The aggregation process then groups hours in which the same combination of demand and generation occur. In the optimisation problem each combination will constitute a period m to be evaluated along with other combinations M. The maximum number of periods to be evaluated will be the product of the number of bins from each series. The occurrence of each combination determines the overall duration τ_m for which it applies – the 'coincident hours'. For instance, in the wind-demand case from Fig. 1(b), there are 49 possible combinations (7 × 7 bins) and the orange blocks indicate hours where demand is 70% of peak and wind is 10%; these conditions occur for a total of 6 h in this case. The process goes through each possible combination and sums the occurrences. Fig. 1(c) shows the resulting number of hourly occurrences for the two-day window indicating some combinations where there are more occurrences and a lot where there are no instances. When carried out over a much longer time series, the process captures the full range of generation-demand combinations. Discretisation does reduce the accuracy of the analysis but only by a few percent, and small compared to uncertainties associated with other planning stage factors (e.g. costs,

locations, and demand growth). Importantly, it does retain the extreme cases (e.g. maximum generation, minimum demand and vice versa) which are critical in driving network constraints.

Fig. 1(a)-(c) shows the case for a single resource and demand time series, providing a bivariate distribution of occurrence. When an additional resource is added, the process remains the same but three-way combinations are defined for each resource and demand. For example, as in this paper where there is wind and PV, the result is a tri-variate distribution of occurrences. This is more challenging to illustrate, but Fig. 1(d) shows how the combinations are handled – this effectively results in a stack of wind-demand combinations arranged by PV output level.

2.5. Implementation

The methods were implemented using the AIMMS optimization modelling environment [31] using the CONOPT 4.0 NLP solver to solve the nonlinear programming formulation of the multi-period multi-resource OPF. Analysis with a single renewable type took 5 min and hybrid combinations around 30 min. The generic problem formulation given here can be coded in any optimisation software (e.g. General Algebraic Modelling System, MATLAB) and there are open source NLP solvers available, e.g. IPOPT. The modelling of renewable variability through discretisation and aggregation to reduce computational complexity (Section 2.4) is independent from the choice of software and solver.

3. Case study

The case study considers the connections of multiple co-located hybrid wind and PV generators across a representative distribution network in order to identify the value of diverse resources and active network management on the effective use of network capacity. The network is representative of UK systems but the analysis process will be
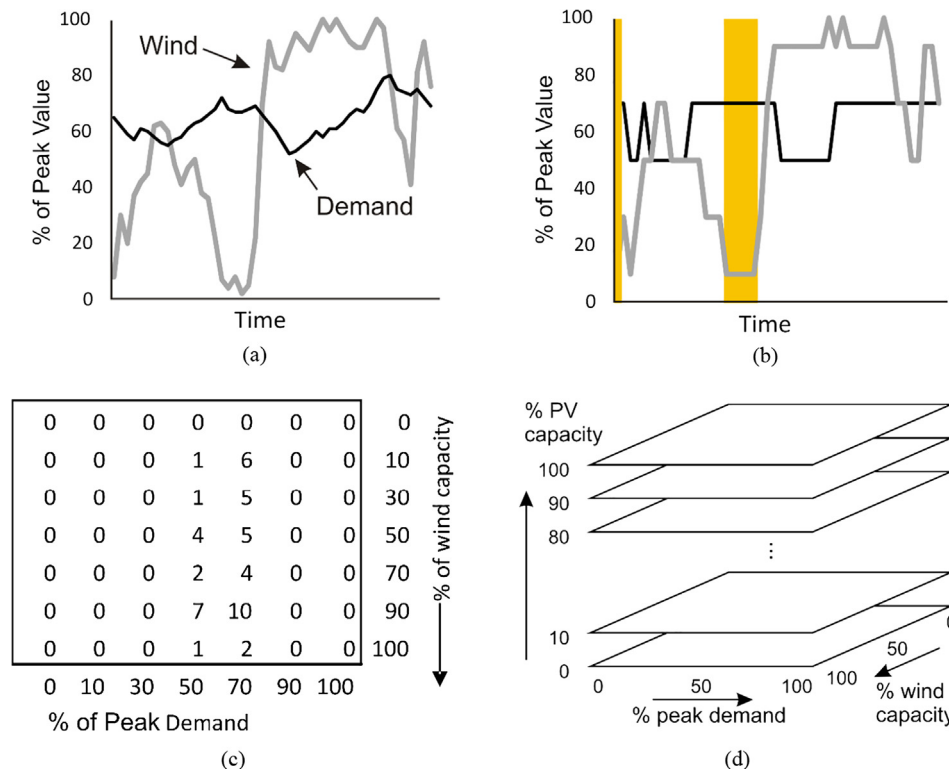

Fig. 1. (a) Normalised hourly demand and wind power time series; (b) discretised wind and demand time series; (c) all aggregated wind-demand combinations showing 'coincident hours'; (d) visualisation of PV-wind-demand combinations.

applicable elsewhere.

3.1. Distribution network

The EHV1 Network from the UK Generic Distribution System is used as the study case (see Fig. 2). Full data for this 61-bus 33/11-kV weakly-meshed rural network are available in [32]. Two identical 30-MVA 132/33-kV transformers connect to the transmission network and supply the feeders with total peak demand of 38.2 MW. The upstream GSP voltage is assumed to be nominal. In the traditional network case that operates without active network management (termed the 'passive' network), the substation OLTC operates to maintain a target voltage of 1.045 p.u. at the lower voltage bus (bus 302). The OLTCs on the 33/11-kV distribution transformers and voltage regulators have a target voltage of 1.03 p.u. In line with UK regulations, all 11 and 33 kV voltages are to be maintained within ± 6%.

Six example locations are selected to co-locate wind and PV connections. They are considered sufficiently close geographically such that the same wind and PV time series apply, although this can be extended to consider site specific series. Three different renewable mixes are considered at each site: wind-only, PV-only and hybrid wind-PV. It is important to point out that in the hybrid case, the optimisation may opt to only build generation capacity of one renewable at some or all locations. The analysis of available capacity is first analysed under firm connections in a 'passive' network case to focus on the complementary value of wind-PV. Following that, active network management is considered to investigate the combined benefits.

3.2. Electricity demand

Hourly demand data from Scotland is used in all simulations. The load factor of this demand profile is 0.63. The whole year demand variation is illustrated in Fig. 3 with load in summer relatively lower than winter. Most of the demand occurs within a range of 60–80% of peak demand with peak demand experienced for 83 h over the whole year, similar to the lowest level of 110 h (around 40% of peak).

3.3. Wind and PV resource

The analysis uses information on wind and solar PV resource for a location in Northeast Scotland (57°N and 3°W) to simulate the generation output. The same time period is used for wind, solar and demand data (i.e. co-temporal) to ensure that the key hourly and seasonal patterns and interrelationships between the data are appropriately captured.

Simulated wind and solar radiation time series data is used for the analysis as measured generation data is not always available due to confidentiality, at the locations of interest or, available for both resource types at the same location. Both the wind and solar simulation approaches are based on high quality datasets that have been well validated, and the general approaches are now well-established and in use in academic, consulting and industry work. The approach means that the location can be varied should the analysis need to be repeated elsewhere.

The wind generation time series is created from the output of a high resolution mesoscale meteorological modelling approach described in [33]. This employed the Weather Research and Forecasting Model and
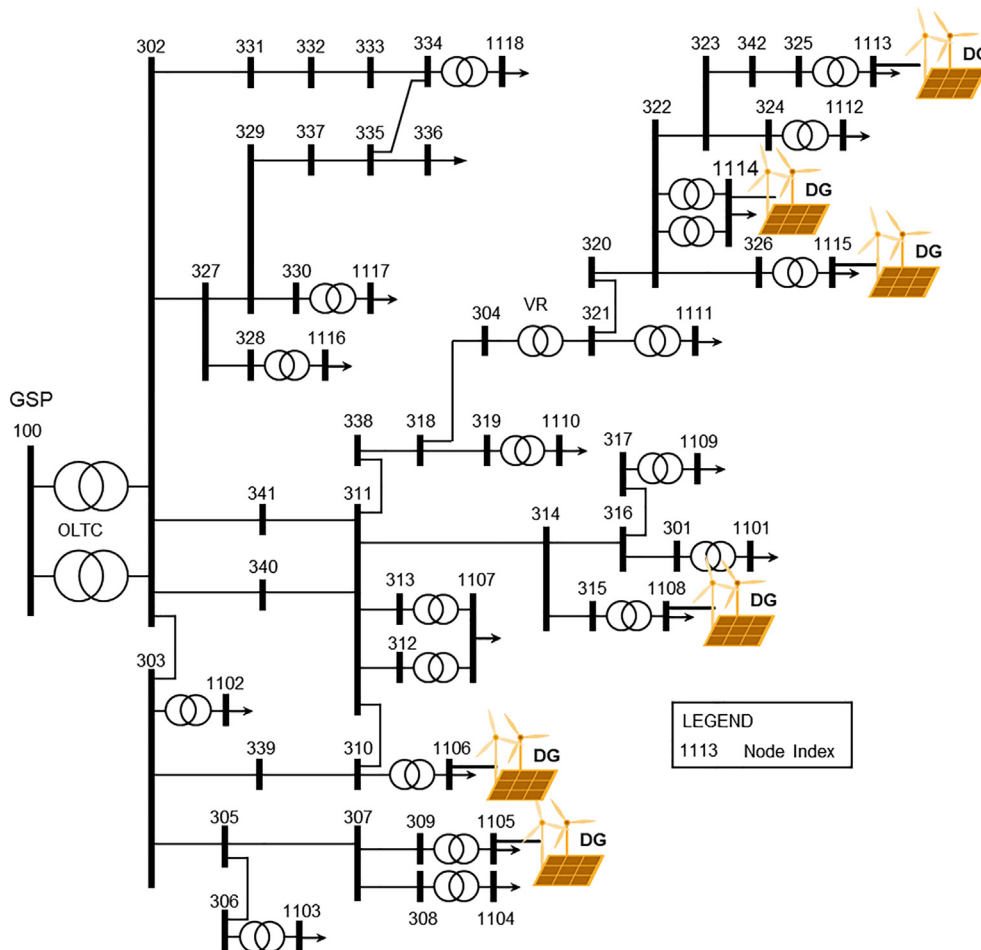

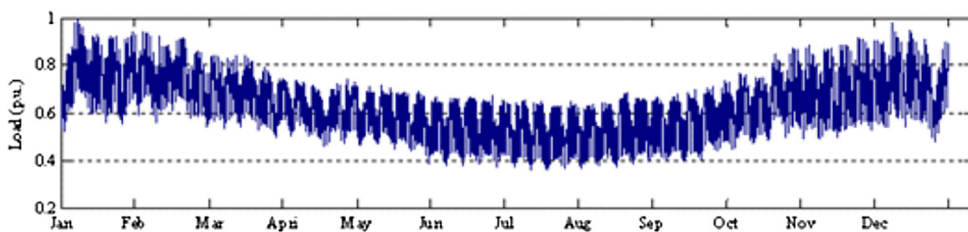Fig. 2. UK GDS EHV1 Network and potential locations for hybrid generation.

Fig. 3. Hourly demand variation for Scotland.

the UK national supercomputer to create a hindcast from the NCEP Global Forecast System. The hourly data covered the whole of the UK and Ireland at 3 km resolution for the years 2000–2010. It is validated against measured data from many UK Met Office met stations, on– and offshore wind mast data and offers wind speed estimates that offer low bias and high correlation. The power production time series was generated using wind speed data from 80 m height along with the power curve of a 3 MW Vestas V90 wind turbine. The resulting power time series have been validated against individual wind farm and national aggregate generation time series.

The solar PV time series is created from the Satellite Application Facility on Climate Monitoring (CMSAF) dataset using the approach as described in [34]. CMSAF employs EUMETSAT geostationary satellite data to estimate key irradiance values and provides data on an hourly basis on a 0.05° latitude and longitude grid (approximately 4 km) for 1983 to 2015. The global horizontal irradiance has been validated against UK Met Office met station data, showing low bias and high correlation. The PV generation data is modelled using well established trigonometric and PV cell relationships. A typical mono-silicon PV panel installation (~16% standard efficiency, 35° tilt, southerly orientation, and 96% inverter efficiency) is adopted to calculate the solar PV output time series; these have been validated against available solar PV output from a range of installations.

Data for the 2008 year are used for illustration. The resulting capacity factors are approximately 37% for wind and 12% for PV; these are credible for a windy site in Scotland. While the PV resource is not as good as wind in terms of overall capacity factor in this area, complementarity still exists between wind and PV as the cross-correlation is −0.13, indicating a relatively low and slightly negative correlation, suggesting low likelihood of high production at the same time. In addition to the specific location used in the case study, several other locations in Scotland were examined prior to application to the electrical modelling. These differed in terms of the specific level of wind and solar resource as well as their coincidence, and while these effects would

have come through in the analysis, they were not regarded as large enough to substantially change the overall picture.

To simplify the presentation and simulation, the levels of wind and PV generation are normalised (per unit) against peak values. The seasonal pattern is illustrated through monthly box plots shown in Fig. 4. Sample time series of wind, PV and demand during a winter and summer month is given in Fig. 5.

3.4. Coincidence of hybrid renewables and demand

The hosting capacity of hybrid DG is largely determined by the 'coincidence' between multiple types of renewable generation and demand. When high levels of generation occur with low local demand, it is most likely to impose constraints on the network as a result of the export of power towards the GSP.

The coincidence of individual renewables and demand is analysed first as the basis for comparison. Adopting the discretisation-aggregation process described in Section 2.4, the time-series of demand, wind and PV generation levels are discretised into bins relative to maximum values with bin values based on the upper values of the ranges: ten ranges for demand ([0,10%], (10%,20%], …), and 11 each for wind and PV (e.g.,{0}, (0,10%], (10%,20%], …).

Fig. 6 shows the coincident hours (i.e. the bivariate distribution) for separate cases of wind and PV with demand. Of the 110 possible combinations of wind and demand, only 69 have a non-zero number of hours; similarly, of the 110 for PV and demand, 52 are non-zero. Many of the combinations with no instances arise from demand always exceeding 40% of peak. There are relatively few instances where peak generation occurs at high demand levels, particularly so for PV as insolation levels will be low in winter. Similarly generation levels are weighted towards lower levels, specifically for PV. Of most importance for hosting capacity is the occurrence of high generation availability and low demand as this promotes energy export and voltage rise. In both cases the occurrence of periods with high generation (80% to
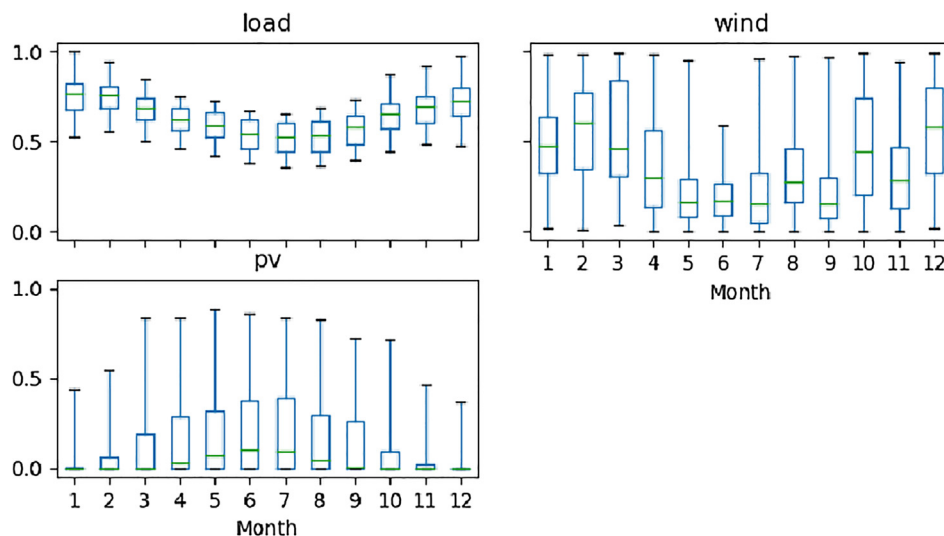

Fig. 4. Monthly boxplot of load, wind and PV output level (p.u.): extremes, median, interquartile range.
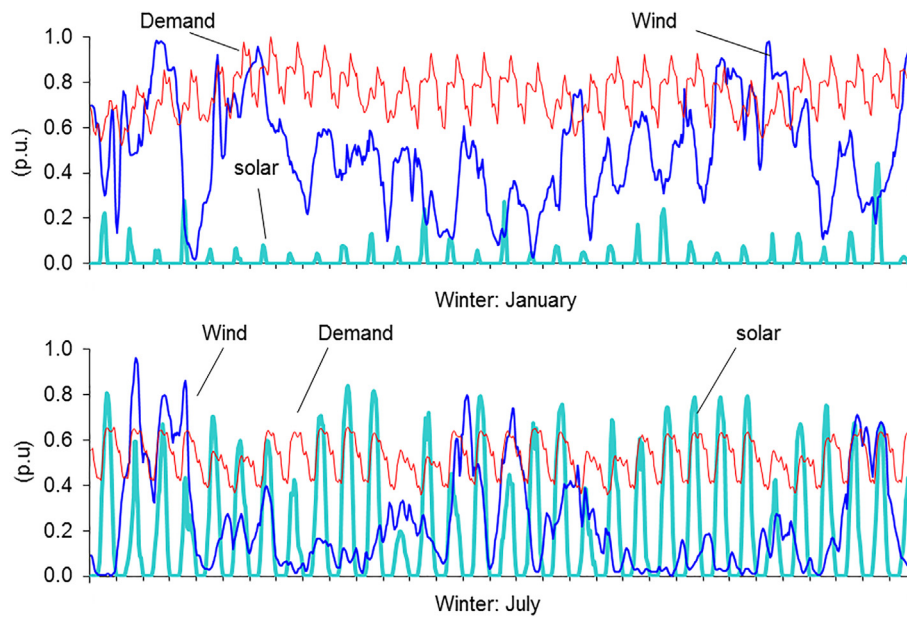
Fig. 5. Time series of wind, PV output and load (p.u.) for winter (top) and summer (bottom) month.

100%) and low demand (40% to 60%) is relatively infrequent over the whole year: 301 h for wind and demand and 33 h for PV and demand, respectively (highlighted in red in Fig. 6). The much lower occurrence of these conditions with PV is due to the minimum load occurring during the night. The hosting capacity determined by such infrequent worst-case scenarios will constrain the network more than is necessary.

The combined (trivariate) coincident hours between wind, PV and demand together are also generated using the approach outlined in Section 2.4. Following the three dimensional model outlined in Fig. 1 (d), the combinations can be visualised as a set of 11 layers of 110 wind-demand cases with a possible total of 1210 PV-wind-demand combinations. However, due to the minimum demand levels and the variability of wind and PV, only 401 cases contain a non-zero number of hours. Fig. 7 illustrates a 'slice' through the distribution with combinations of PV and demand when wind output is 60% of peak: almost half of the potential operational scenarios do not occur. While the trivariate coincidence matrix of wind-PV-demand is obtained, it is challenging to identify the jointly binding worst-case scenario due to all potential network interactions, without use of an optimisation approach such as that proposed here.

3.5. Hybrid hosting capacity in a passive network

The initial hosting capacity evaluation considers that the distribution network operates with no use of active network management (i.e. the 'passive' case). The only control actions in the network are from the transformer tap changers in the GSP substation, voltage regulator and 33/11 kV distribution transformers to maintain their secondary (low) voltage at fixed values ensuring supply on the 11 kV feeders is within voltage limits. The capacity is evaluated for all energy mix cases with the results presented in Table 1.

For individual renewable cases, it can be seen that hosting capacity for the PV-only case is 24% higher than the wind-only case, but the total energy production from PV is only 39% of wind. The difference is partly due to wind's better matching with demand variation than PV in this area as well as the much higher wind capacity factor, requiring less capacity to reach network limits. When PV and wind generation are considered jointly (hybrid), the total annual energy production increases: relative to wind-only the increase is 2% to 127 GWh but compared to PV-only the increase is 162%. The changes in production reflect the underlying changes in capacity: moving from the wind-only

to the hybrid case sees overall capacity increase by 10% with wind capacity reducing slightly (0.5 MW) but with a larger (4.3 MW) amount of additional PV. Moving from PV-only to hybrid sees overall capacity fall by 11%, with PV dropping by over 90%, replaced by a slightly smaller amount of wind. Wind dominates the capacity mix at all sites (90%), mainly because the wind resource has better correlation with demand and high capacity factor. However, it is important to note that PV is part of the optimal result for every connection although in lower amounts. This demonstrates that the complementarity between wind and PV resources is captured by the evaluation approach as a 'benefit' in terms of additional generation.

The different capacities imply different levels of network usage among the three cases. By inspecting the results, voltage rise is identified as the binding constraint in this passive network rather than line overloading. The occurrence of voltages reaching the allowed upper limits at any location in the network is summed for each month as shown in Fig. 8. For the wind-only case, voltage is at the +6% upper bound more frequently during the winter months when wind speeds are higher. For PV-only, the occurrence of high voltages also follows its resource pattern, peaking in July, but much less than wind overall. This illustrates that, in this location, wind uses the network more effectively and is able to generate more energy than PV alone. However, the hybrid wind-PV case (black line in Fig. 8) shows that the occurrence of high voltages is greater than the individual wind and PV cases, indicating that the capacity of the network is being used more effectively by a diverse portfolio. The exception is in June, when PV-only makes more use of the network; the reduction in the hybrid case is as a result of smaller PV capacity but is more than compensated by increases in the rest of the year.

The optimal DG capacities exhibit substantial differences across the six locations, as Fig. 9 shows. As these are voltage-limited, the capacity is broadly distributed according to the electrical distance to the GSP substation, with nearer sites having more capacity available. In cases where the sites share a section of feeder, there is also a trade-off between these that favours closer connection. The effect is most apparent with wind where the voltage constraints are more active. For the hybrid case, the allocations between wind and PV also differ between locations, with PV capacity at bus 1115 twice at that at bus 1106 despite their wind capacity being nearly the same. This is due to the network topology compounding the effect of diversity and is difficult to evaluate without an approach such as that employed here. Overall, the results
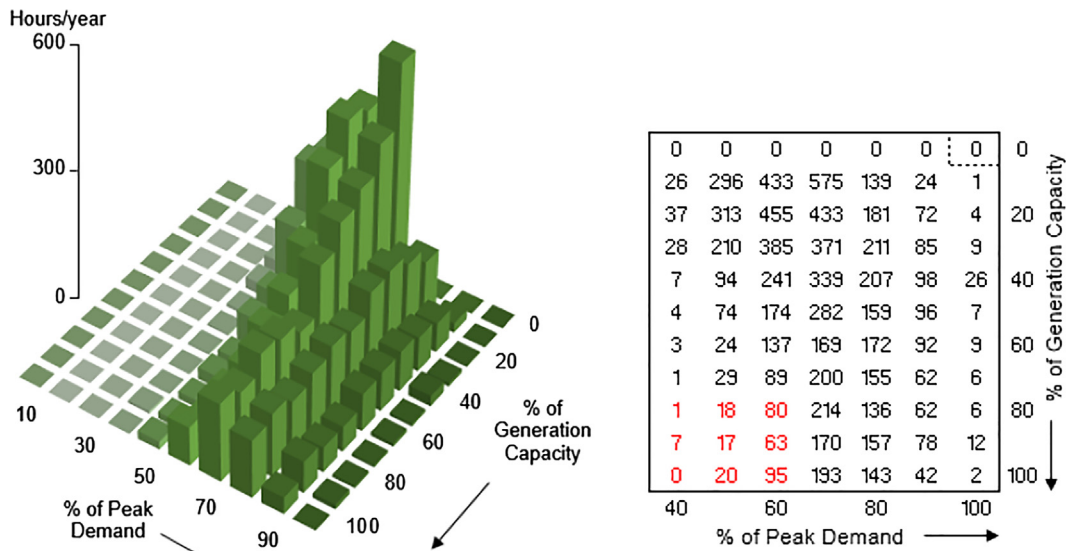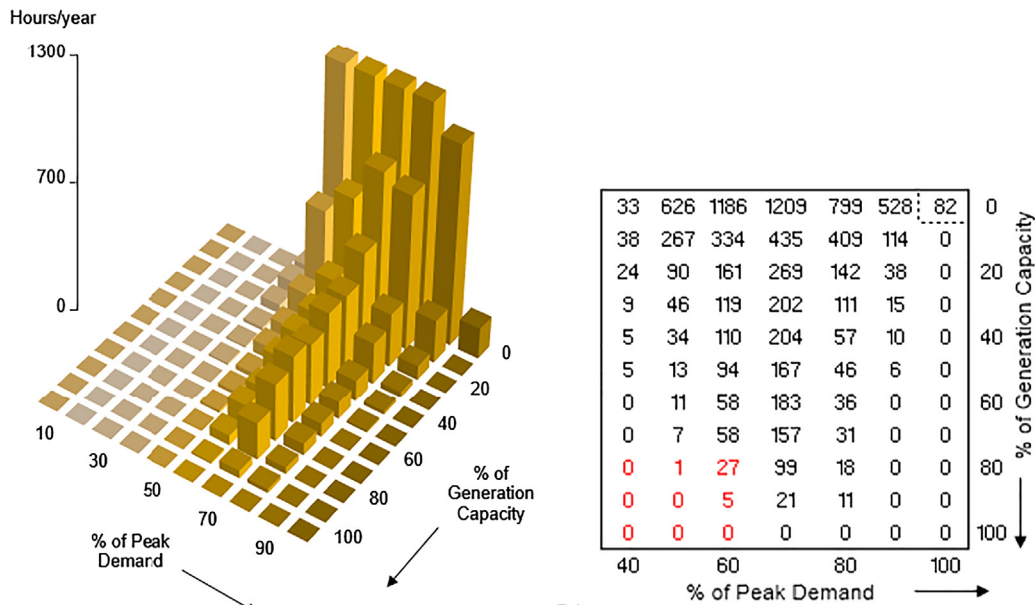
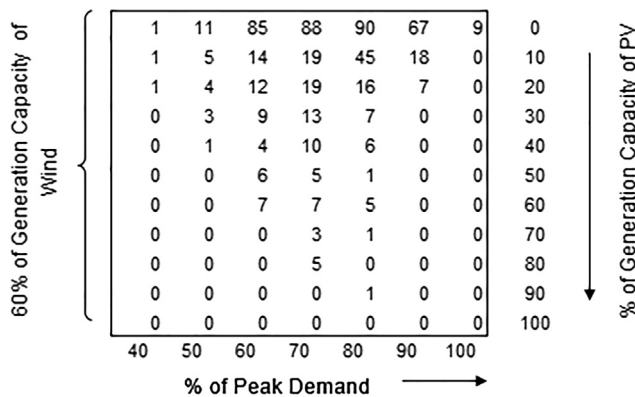Fig. 6. Coincident hours for (a) wind-demand and (b) PV-demand scenarios.

Fig. 7. Example of the coincident hours for PV and demand with wind output at 60% of peak.

Table 1
Hosting capacity for different energy mixes in a 'passive' network.

	Wind only	PV only	Hybrid
Wind capacity (MW)	37.6	–	37.1
PV capacity (MW)	–	46.7	4.3
Total hosting capacity (MW)	37.6	46.7	41.4
Total delivered generation (GWh/year)	124.1	48.6	127.2
Equivalent capacity factor (%)	37.7	11.9	35.1

from the 'passive' case show that network capacity analyses that ignore the effect of resource diversity may be overly conservative, limiting the ability of generators to be used to best effect.

3.6. Hybrid hosting capacity in an actively managed network

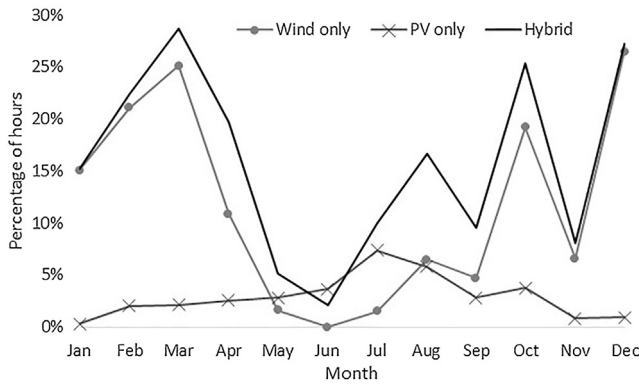The network value of hybrid DG is analysed once more using active

Fig. 8. Occurrence of high voltage hours per month for passive network.
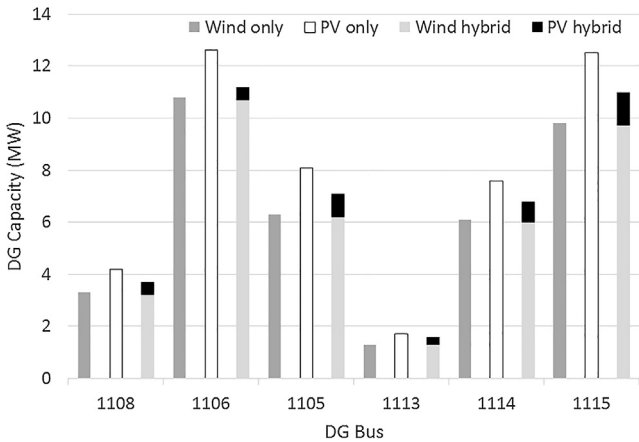

Fig. 9. Hosting capacity allocation for different locations for passive network.

network management schemes to investigate the combined impact of hybrid generation and ANM in improving network utilisation and renewable production.

For adaptive voltage control, the transformer tap changers and voltage regulator are dynamically controlled, with the voltage on their (low voltage) secondary side set optimally in each period within a ± 6% range. For active output control, the simplified approach to handling principles of access governing curtailment means it is assumed that all DGs are available to be curtailed if necessary. In the hybrid case, the amount of curtailment for each period is optimally defined for wind and PV for each location individually. For illustration, curtailment for *each* site was limited to 10% of its total potential energy generation over the year, which is a function of its capacity. The effect of alternative assumptions about curtailment are considered in Section 3.7.

The resulting capacity and energy production are presented in Table 2. Looking at the ANM case in isolation, capacity in the hybrid case increases by 70% relative to wind-only and by 30% relative to PV-only. The energy production benefits are 13% relative to wind-only but 183% relative to PV-only. These changes are considerably larger than the equivalent for the passive network. Comparison with the passive cases (Table 1), shows that both individual and hybrid renewable cases see increased energy production and more available capacity: wind-only sees growth of 74% in capacity and 56% in energy, PV-only sees an additional 78% capacity and 60% energy and, most notably, the hybrid case sees capacity increase by 162% with energy up 73%. The more balanced capacity split between renewables in the hybrid case with ANM is clear (PV is now ∼46% of the total, up from 10% in the passive case) and shows the real value of active control in facilitating new connections with more diverse resources. The capacity distribution among different connection locations also shows significant differences (Fig. 10). For single resources, capacity at individual buses increases by

between 64% and 85% for wind, and 76 to 80% for PV. The hybrid cases see relative increases of between 144% and 163%. The large increases in capacity are driven by selective use of curtailment with the optimisation raising capacity until 10% reductions in total production are seen for each location. This reduces the average capacity factors across the sites to 34% for wind, 10.7% for PV and 23.2% for the hybrid combination. The low capacity factor in the hybrid case is simply a feature of a large proportion of PV in the mix.

With ANM, the voltage-rise issue that was apparent in the passive network cases is largely solved by actively lowering the secondary voltage of the transformers to reduce the voltage across the network. As such, the binding network constraint for the ANM cases switches to the power flow limits of lines and transformers. In many cases this is the limit of the 33/11 kV transformers located close to the DG. The occurrence of high line-loading (any line or transformer with loading > 98%) in each month is shown in Fig. 11, indicating the utilisation of network capacity. While all three renewable cases show increased usage of the network to export energy than the passive case (where no line reached 98% of limits), the hybrid case shows more utilisation of network in almost every month. By isolating the infrequent periods of very high joint output, more 'balanced' hybrid renewable generation allows smoother output with less variability in other periods, and therefore more effective use of network capacity.

3.7. Impact of curtailment rules

With ANM, levels of curtailment for a particular DG depend strongly on the principles of access (as mentioned in Section 2.3.2), which govern the sharing of curtailment according to predefined rules. The analysis has simplified this aspect but the framework can be used to examine the effect in broad terms by varying the assumptions underpinning allowable levels of curtailment.

The main analysis in Section 3.6 uses the assumption that a maximum 10% of *total production from each site* may be curtailed. The analysis was repeated with two alternative settings for allowable curtailment levels, in order to better understand how curtailment may be shared:

- Alternative A applies a stricter limit on curtailment and restricts curtailment to a maximum of 10% *per renewable per site*;
- Alternative B applies a looser constraint and restricts overall curtailment to 10% across *all sites*, enabling the optimisation to choose the most appropriate amount of capacity and curtailment between wind and PV as well as among DGs.

The results from these analyses are given in Table 3 for the initial case and the alternatives. These show the alternative cases have optimal capacities and resource distributions that are very close to the initial case. Alternative A is generally the same to one decimal place with Alternative B has around 0.2 MW greater overall capacity (< 0.2% change) as a result of greater 'freedom' for the algorithm to choose between sites. The primary reason for the similarity is that as the main constraint is at the transformers close to the DG, there is limited scope to trade-off between resources and sites. Other networks may behave differently.

Table 2
Hosting capacity and energy production with active network scheme.

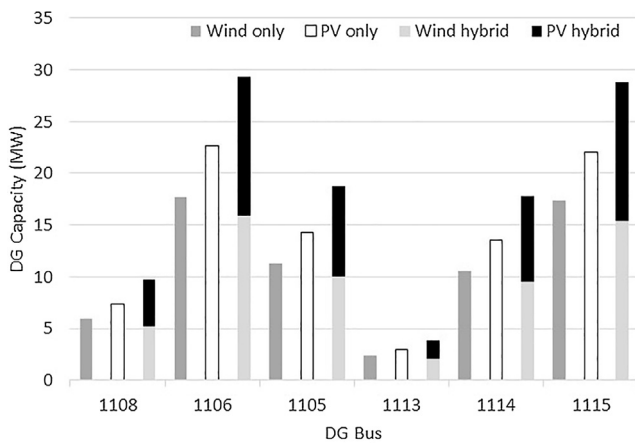|	Wind	PV	Hybrid
Wind capacity (MW)	65.2	–	58.1
PV capacity (MW)	–	83.0	50.1
Total hosting capacity (MW)	65.2	83.0	108.2
Total delivered energy (GWh)	193.9	77.7	219.8
Total curtailed energy (GWh)	21.5	8.6	24.4
Equivalent capacity factor (%)	34.0	10.7	23.2

Fig. 10. Hosting capacity allocation for different locations with active network.
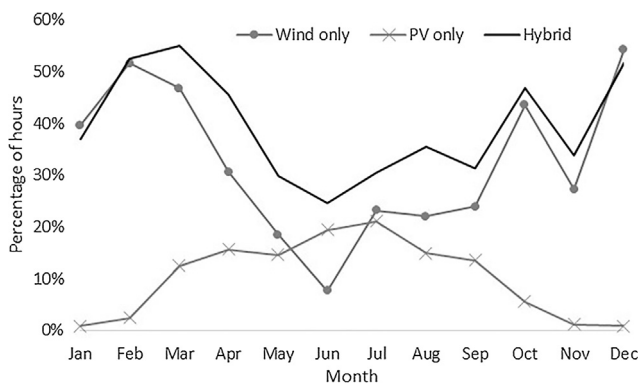

Fig. 11. Occurrence of high line loading hours in each month with active network.

Table 3
Hosting capacity with different curtailment rules for active network scheme.

	Initial case	Alternative A	Alternative B
Wind capacity (MW)	58.1	58.1	58.0
PV capacity (MW)	50.1	50.1	50.4
Total hosting capacity (MW)	108.2	108.2	108.4
Total delivered energy (GWh)	219.8	219.7	219.6
Total curtailed energy (GWh)	24.4	24.4	24.4
Wind energy curtailed (%)	6.5	10.0	6.8
PV energy curtailed (%)	23.0	10.0	21.6

The most significant result is that while the overall change in curtailment volume is virtually zero, there are notable differences in terms of the relative amounts of curtailment of wind and PV. The main case allows site level optimisation and tends to curtail wind on average by 6.5% over the sites but curtails PV by 23% on average. By contrast, alternative A imposes a resource-level constraint with all sites constraining wind and PV to 10%, in effect reducing PV curtailment by at least half but increasing wind curtailment by 50%. Alternative B has more freedom and constrains wind on average by 6.8% and PV by 21.6%, slightly less extreme than the initial case. There is also some variation between sites between the 3 cases: curtailment is uniform in Alternative A; it varies by 5.6–7.9% for wind and 17.5–26% for PV in the initial case; and by 6.2–8.2% for wind and 15.9–23.9% for PV for Alternative B. The outcome of this analysis is that the level of curtailment for individual sites and technologies is very sensitive to the underlying assumptions. In particular, it suggests that despite no net gain overall there could be substantial negative impacts on one technology and suggests that equitable solutions are required to avoid disproportionate outcomes.

4. Discussion

This work examined the value of hybrid combinations of renewable DGs in terms of being able to better use the capacity of the distribution network for generating and exporting renewable energy, in this case with wind and PV. This is understood to be the first analysis to specifically link diversity of supply to use of network capacity in this manner. The diversity in timing between solar and wind output is seen to be useful in driving this. However, it is important to emphasise that the network will still be constrained by critical periods of joint maximum production and low demand. Therefore, if renewable resources reach their peak around the same time (e.g. strong wind during a summer day), even for very few periods of the year, the benefit of complementarity over the other periods is reduced. This explains the limited 'value' of diversity from hybrid DG seen in the passive network case. Implementation of advanced network control to actively manage constraints during these critical periods was anticipated to add significant value for the grid integration of hybrid DG. It was clear from the case study that there were major increases in network capacity and energy production arising from ANM across the single resource and hybrid cases. In addition, it was seen that ANM significantly enhanced the benefit of diversity between wind and PV, relative to the passive cases.

The relatively high winds and low insolation in Scotland is likely to have influenced the 'value' of diversity in supplies. It might be expected that the value of hybrid DG in increasing network utilisation and total energy export would be strengthened in areas where the wind and PV resources are more comparable. In saying that, the insight gained from the case study can be generally transferred to other networks and there would be scope to expand the scope of the analysis to other areas and alternative combinations of resources. The choice of most appropriate ANM technology for different networks needs separate, detailed study, but in general, adaptive voltage control is a useful option where the voltage issue solely constrains the network, while curtailment can, at least partially, solve both voltage rise and power flow issues.

There are two main applications of the approach. The first, as employed in this paper, compares 'optimal' combinations of resources at particular sites and this would be directly applicable to developments in undeveloped (or 'greenfield') networks where it can be used to identify appropriate shares of capacity at specific locations to guide patterns of development of different renewables. In practice, DG is rarely located optimally so the second application would be in networks where there is existing generation of a dominant technology type. There may be additional capacity available for renewables that exhibit different characteristics to the dominant resource. In this case, the approach can be used by modelling pre-existing generation with fixed capacities but variable production and the 'spare' capacity identified by optimising the remaining capacity with the complementary technology. This is especially valuable in areas, such as parts of the UK, where networks are considered largely 'full' as a result of dominant connections from single resource types.

The ability to exploit complementarity between resources is strongly dependent not only on the technical feasibility but also the economic feasibility. This is governed by the capital and operating costs but also potential revenues which can be negatively influenced by curtailment levels. With ANM, levels of curtailment for a particular DG depend strongly on the principles of access. Ultimately these govern how curtailment is to be shared between DGs and can take a number of forms, including proportional sharing as well as those based on the order of connection with earlier connections having priority over later connections (termed 'last-in-first-out'). For example, where such arrangements are in force, PV aiming to connect to a wind-dominated distribution network may be curtailed more severely than wind. The analysis in Section 3.7 was useful in showing how changes in curtailment 'sharing' drove how technologies were curtailed and where. The analysis showed that there is scope for quite different outcomes for

individual DG, some of which were potentially detrimental. The economics of the different technologies and potential subsidy regimes will therefore play a big role in determining if such 'spare' capacity is exploitable.

The case study employed wind and PV generation time series based on modelled data; the overall analysis would work equally well with measured resource or generation data. The analysis can also be extended to other renewable resource types. The analysis shown here employs a single year of wind and PV data which will tend to reduce the variability in conditions that might be experienced in practice over the life time of the DG. However, the coincidence technique is very well-suited to extended lengths of time series as it will reduce the resulting series to a small number of representative multi-periods. This is an active area of research with a number of useful contributions in recent years, e.g. [35].

Availability and use of storage and demand side management, would also help hybrid DGs to exploit 'spare room' in the network by time-shifting power away from conditions that result in binding constraints. While not examined in this paper, such analysis would be valuable but is more computationally challenging given the temporal dependency introduced by storage, which precludes use of the representative periods technique employed in this paper.

5. Conclusions

Hybrid combinations of resources are recognized as a strategy for handling the variability of renewables. This paper studies the grid integration of hybrid renewable generation from the point of view of efficient use of network capacity. A multi-period, multi-resource AC optimal power flow approach is used to optimally identify the network value of hybrid distributed generation connections in maximising total energy production whilst complying with network operational limits. The effectiveness of hybrid distributed generation and the optimization method was examined through comparison with single resource systems. This study demonstrates that by capturing the complementarity between different renewables helps hybrid distributed generation to better exploit available network capacity, enabling more renewable generation capacity to connect and so raise energy output. In addition, the efficient use of network from hybrid distributed generation becomes more pronounced when active network management is involved, which isolates the infrequent co-occurrence of high outputs.

The network value of hybrid distributed generation is complicated by network topology, the degree of synergy between renewables and correlation with local demand. The evaluation approach presented in this paper allows rapid identification of network-wide benefit of hybrid distributed generation and the combined value with smart grid controls. It can facilitate the wide deployment of hybrid generation in the electricity network to promote renewable generation, carbon reduction and offers assistance in choosing the appropriate active network management technology to enhance hybrid generation in different networks.

Acknowledgements

References

[1] World Energy Outlook 2018. OECD; 2018. doi:10.1787/weo-2018-en.

[2] Lopes JAP, Hatziargyriou N, Mutale J, Djapic P, Jenkins N. Integrating distributed generation into electric power systems: A review of drivers, challenges and opportunities. Electr Power Syst Res 2007;77:1189–203. https://doi.org/10.1016/j.epsr.2006.08.016.

[3] Jenkins N, Strbac G, Ekanayake J. Distributed generation. Institution of Engineering and Technology; 2010.

[4] Keane A, Ochoa LF, Borges CLT, Ault GW, Alarcon-Rodriguez AD, Currie RAF, et al. State-of-the-art techniques and challenges ahead for distributed generation planning and optimization. IEEE Trans Power Syst 2013;28:1493–502. https://doi.org/10.1109/TPWRS.2012.2214406.

[5] Anaya KL, Pollitt MG. Options for allocating and releasing distribution system capacity: Deciding between interruptible connections and firm DG connections. Appl Energy 2015;144:96–105. https://doi.org/10.1016/J.APENERGY.2015.01.043.

[6] Monforti F, Huld T, Bódis K, Vitali L, D'Isidoro M, Lacal-Arántegui R. Assessing complementarity of wind and solar resources for energy production in Italy. A Monte Carlo approach. Renew Energy 2014;63:576–86. https://doi.org/10.1016/j.renene.2013.10.028.

[7] Bett PE, Thornton HE. The climatological relationships between wind and solar energy supply in Britain. Renew Energy 2016;87:96–110. https://doi.org/10.1016/j.renene.2015.10.006.

[8] Hoicka CE, Rowlands IH. Solar and wind resource complementarity: Advancing options for renewable electricity integration in Ontario, Canada. Renew Energy 2011;36:97–107. https://doi.org/10.1016/j.renene.2010.06.004.

[9] Liu Y, Xiao L, Wang H, Dai S, Qi Z. Analysis on the hourly spatiotemporal complementarities between China's solar and wind energy resources spreading in a wide area. Sci China Technol Sci 2013;56:683–92. https://doi.org/10.1007/s11431-012-5105-1.

[10] Deshmukh MK, Deshmukh SS. Modeling of hybrid renewable energy systems. Renew Sustain Energy Rev 2008;12:235–49. https://doi.org/10.1016/J.RSER.2006.07.011.

[11] Arabali A, Ghofrani M, Etezadi-Amoli M, Fadali MS. Stochastic performance assessment and sizing for a hybrid power system of Solar/Wind/Energy Storage. IEEE Trans Sustain Energy 2014;5:363–71. https://doi.org/10.1109/TSTE.2013.2288083.

[12] Nogueira CEC, Vidotto ML, Niedzialkoski RK, de Souza SNM, Chaves LI, Edwiges T, et al. Sizing and simulation of a photovoltaic-wind energy system using batteries, applied for a small rural property located in the south of Brazil. Renew Sustain Energy Rev 2014;29:151–7. https://doi.org/10.1016/J.RSER.2013.08.071.

[13] Xu L, Ruan X, Mao C, Zhang B, Luo Y. An improved optimal sizing method for wind-solar-battery hybrid power system. IEEE Trans Sustain Energy 2013;4:774–85. https://doi.org/10.1109/TSTE.2012.2228509.

[14] Zhao B, Zhang X, Li P, Wang K, Xue M, Wang C. Optimal sizing, operating strategy and operational experience of a stand-alone microgrid on Dongfushan Island. Appl Energy 2014;113:1656–66. https://doi.org/10.1016/j.apenergy.2013.09.015.

[15] Shang C, Srinivasan D, Reindl T. An improved particle swarm optimisation algorithm applied to battery sizing for stand-alone hybrid power systems. Int J Electr Power Energy Syst 2016;74:104–17. https://doi.org/10.1016/j.ijepes.2015.07.009.

[16] Roberts JJ, Marotta Cassula A, Silveira JL, da Costa Bortoni E, Mendiburu AZ. Robust multi-objective optimization of a renewable based hybrid power system. Appl Energy 2018;223:52–68. https://doi.org/10.1016/j.apenergy.2018.04.032.

[17] González A, Riba J-R, Rius A, Puig R. Optimal sizing of a hybrid grid-connected photovoltaic and wind power system. Appl Energy 2015;154:752–62. https://doi.org/10.1016/J.APENERGY.2015.04.105.

[18] Akram U, Khalid M, Shafiq S. Optimal sizing of a wind/solar/battery hybrid grid-connected microgrid system. IET Renew Power Gener 2018;12:72–80. https://doi.org/10.1049/iet-rpg.2017.0010.

[19] Kirmani S, Jamil M, Akhtar I. Economic feasibility of hybrid energy generation with reduced carbon emission. IET Renew Power Gener 2018;12:934–42. https://doi.org/10.1049/iet-rpg.2017.0288.

[20] Di Somma M, Graditi G, Heydarian-Forushani E, Shafie-khah M, Siano P. Stochastic optimal scheduling of distributed energy resources with renewables considering economic and environmental aspects. Renew Energy 2018;116:272–87. https://doi.org/10.1016/j.renene.2017.09.074.

[21] Chowdhury, Crossley, Chowdhury. Microgrids and active distribution networks. The Institution of Engineering and Technology; 2009. doi:10.1049/PBRN006E.

[22] Hu Z, Li F. Cost-benefit analyses of active distribution network management, part I: Annual benefit analysis. IEEE Trans Smart Grid 2012;3:1067–74. https://doi.org/10.1109/TSG.2012.2205412.

[23] Salih SN, Chen P. On coordinated control of oltc and reactive power compensation for voltage regulation in distribution systems with wind power. IEEE Trans Power Syst 2016;31:4026–35. https://doi.org/10.1109/TPWRS.2015.2501433.

[24] Ochoa LF, Dent CJ, Harrison GP. Distribution network capacity assessment: Variable DG and active networks. IEEE Trans Power Syst 2010;25:87–95. https://doi.org/10.1109/TPWRS.2009.2031223.

[25] Capitanescu F, Ochoa LF, Margossian H, Hatziargyriou ND. Assessing the potential of network reconfiguration to improve distributed generation hosting capacity in active distribution systems. IEEE Trans Power Syst 2015;30:346–56. https://doi.org/10.1109/TPWRS.2014.2320895.

[26] Li Y, Feng B, Li G, Qi J, Zhao D, Mu Y. Optimal distributed generation planning in active distribution networks considering integration of energy storage. Appl Energy 2018;210:1073–81. https://doi.org/10.1016/j.apenergy.2017.08.008.

[27] Palensky P, Dietrich D. Demand side management: Demand response, intelligent energy systems, and smart loads. IEEE Trans Ind Informatics 2011;7:381–8. https://doi.org/10.1109/TII.2011.2158841.

[28] Harrison GP, Wallace AR. Optimal power flow evaluation of distribution network capacity for the connection of distributed generation. IEE Proc - Gener Transm Distrib 2005;152:115. https://doi.org/10.1049/ip-gtd:20041193.

[29] Kane L, Ault G. A review and analysis of renewable energy curtailment schemes and principles of access: Transitioning towards business as usual. Energy Policy 2014;72:67–77. https://doi.org/10.1016/j.enpol.2014.04.010.

[30] Boheme T, Taylor J, Wallace AR, Bialaek J. Matching renewable electricity generation with demand. Edinburgh: Scottish Executive; 2006.

[31] Bisschop J. AIMMS optimization modeling. Lulu. com; 2006.
[32] Strbac G, McDonald J. United Kingdom generic distribution system 2004.
[33] Harrison GP, Hawkins SL, Eager D, Cradden LC. Capacity value of offshore wind in Great Britain. Proc Inst Mech Eng Part O J Risk Reliab 2015;229:360–72. https://doi.org/10.1177/1748006X15591619.
[34] Thomson RC, Sun W, Harrison GP. Developing a spatially and temporally explicit

solar resource dataset for Great Britain. IET Renew. Power Gener. Conf., Lyngby, Denmark; 2018.
[35] Pfenninger S. Dealing with multiple decades of hourly wind and PV time series in energy models: A comparison of methods to reduce time resolution and the planning implications of inter-annual variability. Appl Energy 2017;197:1–13. https://doi.org/10.1016/j.apenergy.2017.03.051.